Stability Problems, Low-Energy-Recoil Events, and Vibrational Behavior of Point Defects in Metals

Alfred Scholz
Zentralinstitut für Angewandte Mathematik, Kernforschungsanlage Jülich, Jülich, Germany
and
Christian Lehmann
Institut für Festkörperforschung der Kernforschungsanlage Jülich, Jülich, Germany
(Received 8 February 1972)

In a copper crystallite containing many hundreds of atoms the static and dynamic behavior of point defects is simulated by means of an electronic computer. This follows the lines of an earlier work by Gibson *et al.* We have extended their investigation to collisions with subthreshold energies using a new computer program particularly suited for low-energy processes. The atomic interaction is approximated by a purely repulsive Born-Mayer potential together with surface forces applied to the boundary of the crystallite. The mechanical equilibrium of vacancy, interstitial, and many Frenkel-pair configurations has been determined. There are 74 lattice sites around a (split) interstitial which are unstable for a vacancy. The formation energy (2.79 eV) of a stable Frenkel pair turns out to be practically independent of the distance between vacancy and interstitial. The effect of subthreshold collisions on point defects has been studied. At low-energy transfers ($\lesssim 0.3$ eV) only vibrations can be excited. The (split) interstitial exhibits several localized modes: (i) an axial vibration, (ii) a twofold degenerate librational mode, and (iii) a twofold degenerate c. m. oscillation perpendicular to the axis. The energy storage in the axial mode is about 20% of the initial energy transfer. Jumps of point defects are induced by energy transfers of $\gtrsim 0.3$ eV for interstitials and $\gtrsim 0.6$ eV for vacancies. The directional dependence of these energy thresholds has been studied. The cross section for interstitial jumps due to MeV electrons is roughly 10^{+4} b. Effects of subthreshold energy transfers to close Frenkel pairs have also been investigated.

I. INTRODUCTION

Since the study of radiation-induced defects in metals has become an important tool in solid-state physics, one of the basic questions has concerned the elementary process of defect *production*: What is the threshold energy which a lattice atom must be given to be displaced from its lattice site forming a stable interstitial atom and leaving behind a vacancy? Only recently it was considered[1] that not only these above-threshold collisions might cause physical changes in a crystal but also subthreshold collisions. By definition, subthreshold collisions cannot produce defects in an *ideal* crystal. However, in a *defect* crystal they can be effective, for instance by inducing jumps of vacancies and interstitials by energy transfers much smaller than those required for defect production. In an irradiation experiment with, say, copper with low-energy electrons of 0.4 MeV or platinum with electrons of 1.4 MeV this implies that no defects will be created; however, the defects already present can be kicked by the electrons from one equilibrium position to a neighboring one. This "playing soccer" of electrons with interstitials or vacancies phenomenologically resembles thermal diffusion of these defects. There are measurable effects of atomic jumps if they cause a change of the defect state.

Such a change can lead, e.g., to mutual annihilation of vacancies and interstitials, which are close to each other (close Frenkel pairs),[2,3] or to a change of their mutual distance.[3,4] Subthreshold collisions may be important in all collision processes where predominantly small energies are transferred to atoms such as, e.g., in electron microscopy or in channeling experiments. Of course, not only single point defects can be affected but also aggregates like interstitial clusters etc.

Owing to the complexity of experiments in which such effects have been observed it is impossible to trace the basic events on an atomic scale. Hence a calculational approach is highly desirable to interpret experimental data at least qualitatively.

In this approach one has to deal with a complicated many-body problem which requires an electronic computer to simulate the elementary processes taking place in a real lattice. The methods adopted for this purpose are essentially along the lines of earlier computer studies[5] concerning above-threshold events. A new computer program has been set up[6] which is especially suited for studying subthreshold events where most lattice atoms show only very small displacements from their equilibrium positions. This program has been used to investigate the equilibrium configuration (without thermal motion) of a vacancy, an interstitial, or a Frenkel pair in an otherwise

ideal lattice and their response to momentum transfers to a given atom, which may result in a jump of the defect in excitation of vibrational (e.g., localized) modes of an interstitial or in annihilation of a Frenkel pair. All calculations have been performed with an IBM 360/75 computer.

II. CRYSTAL MODEL

A. General Considerations

For simulating subthreshold events in a macroscopic crystal, one actually should treat an infinitely large crystal. Since this is not feasible one has to restrict oneself to treating a "subspace" of an infinite crystal, i.e., a small crystallite of about thousand atoms. In order to be representative for the infinite crystal, equations of motion of the atoms in the small crystallite must contain the interaction with the "rest." The coupling of the crystallite to the "rest" can be restricted to the surface of the crystallite if the atomic interaction is short range. If in addition the displacements of the surface atoms are small as compared to the lattice constant, a lattice-Green's-function formalism could be used in principle in order to describe the reaction of the "rest" exactly. Since this is too complicated one can try to replace a lattice Green's function by an elastic Green's function describing the response of the "rest" by means of elastic-continuum theory. This would be correct if the frequencies involved were in the elastic range. One must keep in mind, however, that the elastic Green's function does not imply a maximum frequency and that, therefore, strictly stationary localized modes would not exist. The elastic Green's function essentially represents three effects: (i) constant forces which compensate surface relaxations of the small crystallite and restore the ideal lattice; (ii) elastic response of the surrounding medium to displacements of boundary atoms; (iii) radiative forces representing the emission of elastic waves originating from atomic motions in the crystallite.

However, even the elastic-Green's-function treatment is still too difficult. Hence, one is left with even cruder approximations:

(a) The attractive forces between atoms [interatomic forces are derived from a central potential $V(r)$] in the crystallite are not treated atomistically but are replaced by boundary forces such that the lattice of the crystallite is maintained. Since we treat only interactions between first and second neighbors, these forces must act on the surface atoms and their first neighbors. Only part of these forces would be contained in the elastic Green's function, namely, the terms compensating surface relaxations.

(b) In an infinite crystal the forces on atom i are given in the harmonic approximation by

$$\vec{K}_i = \sum_k \underline{T}_{ik}(\vec{s}_i - \vec{s}_k) \ .$$

Here the tensor $\underline{T}_{ik}$ represents the harmonic force parameters of the ideal crystal with repulsive and attractive forces, and k runs over all first and second neighbors, i.e., only first and second neighbors are contained in $\underline{T}_{ik}$. The vector $\vec{s}_i$ represents the displacement of atom i.

(c) The force $\vec{K}_i^R$ exerted by the surrounding medium ("rest") on atom i in the crystallite is obtained by summing over the atoms $k = \lambda$ of the rest:

$$\vec{K}_i^R(t) = \sum_\lambda \underline{T}_{i\lambda}(\vec{s}_i - \vec{s}_\lambda) \ . \tag{1}$$

To get a crude estimate of the influence of the rest we assume that atom λ is first neighbor to atom i and that $\vec{s}_\lambda$ is proportional to $\vec{s}_i(t - D/c)$, where D is the first-neighbor distance and c an average velocity of sound:

$$\vec{s}_\lambda(t) = g\vec{s}_i(t - D/c) \approx g[\vec{s}_i(t) - (D/c)\dot{\vec{s}}_i(t)] \ . \tag{2}$$

Inserting (2) into (1) one obtains

$$\vec{K}_i^R = \vec{F}_i^{R,\mathrm{el}} + \vec{F}_i^{R,\mathrm{rad}} \ , \tag{3}$$

where

$$\vec{F}_i^{R,\mathrm{el}}(t) = (1-g)\sum_\lambda \underline{T}_{i\lambda}\vec{s}_i(t) \tag{4}$$

are forces describing the elastic response of the rest on atom i and

$$\vec{F}_i^{R,\mathrm{rad}}(t) = g(D/c)\sum_\lambda \underline{T}_{i\lambda}\dot{\vec{s}}_i(t) \tag{5}$$

are the radiative forces acting on atom i. The proportionality factor g is considered an open parameter between 0.1 and 1.0. The value $g = 1$ represents the case of no elastic interaction with the rest [cf. (4)]. The value $g \approx 0$ corresponds to a fixed atom $\lambda(\vec{s}_\lambda \equiv 0)$ and therefore to rigid rest. It turns out that its value practically does not influence the results. This shows that for all energies used the size of the crystallite is so large that the radiative effects are small. Eventually we obtain for the total force acting on atom i

$$\vec{F}_i = \vec{F}_i^C + \vec{F}_i^R \ , \tag{6}$$

where $\vec{F}_i^C$ is the force exerted by the atoms of the crystallite (only repulsive interaction) and $\vec{F}_i^R$ represents the interaction with the rest. The force $\vec{F}_i^R$ contains three terms:

$$\begin{aligned}\vec{F}_i^R &= \vec{F}_i^{R,\mathrm{const}} + \vec{F}_i^{R,\mathrm{el}} \\ &= \vec{F}_i^{R,\mathrm{const}} + \vec{K}_i^R \ .\end{aligned} \tag{7}$$

The first term is independent of $\vec{s}_i$ and provides the ideal structure of the crystallite. The second term, given by (4), is linear in $\vec{s}_i$, and the third term given by (5), is linear in $\dot{\vec{s}}_i$.

B. Specific Case of Copper

In this paper we treat copper specifically. The atoms form a face-centered lattice (Fig. 1) and are supposed to interact by a purely repulsive potential of the Born-Mayer type, cutoff at $r = r_c$,

$$V(r) = \begin{cases} A(e^{-r/a} - e^{-r_c/a}), & r \le r_c \\ 0, & r \ge r_c \end{cases} \qquad (8)$$

where r is the interatomic distance.

The constant term in (8) just provides a continuous behavior of $V(r)$ at $r = r_c$. Together with the constant surface forces which render the crystallite stable (with the correct lattice constant) the model is not of a purely central-force type and the Cauchy relation for the elastic constants need not be fulfilled. The constants $A = 22.563$ keV and $a = \frac{1}{13}D$, where $D = 2.551$ Å is the nearest-neighbor distance, were taken from earlier[5] calculations. The cutoff distance r_c was taken as $r_c = 1.58D$, allowing for second-neighbor interaction. The constants A and a are believed to be practically independent of slight changes of r_c to which they are linked via physical properties such as elastic moduli. For the cubic cell edge the value $a_0 = D\sqrt{2} = 3.608$ Å corresponding to 0 °K was taken since all pertinent experiments have been performed at very low temperatures.

It should be emphasized that the constants A, a of the potential (8) are such (cf. Ref. 5) that the displacement-energy threshold of copper (≈ 25 eV) is reproduced. Also, the three elastic constants c_{11}, c_{12}, c_{44} are reproduced reasonably well by the potential (8) although it employs only two parameters.

A crystallite of atoms interacting with a purely repulsive potential (8) would not be stable. Therefore, constant forces are applied to the surface atoms to provide stability. However, one has to make sure, that the crystallite not only is stable and shows the correct elastic constants, but also exhibits the right local response. For this reason we have calculated the Einstein frequency, i.e., the frequency of an atom vibrating about its lattice position if all the other atoms are held fixed at their ideal lattice sites. Expansion of the lattice potential up to quadratic terms in the displacement of the vibrating atom yields the force constant f_{BM}. With the mass m of a copper atom, one obtains

$$\omega_E^{(BM)} = (f_{BM}/m)^{1/2} = 2.63 \times 10^{13}\ \text{sec}^{-1}\ . \qquad (9)$$

The corresponding calculation for a Morse potential (the Morse potential was taken from Ref. 7 and corrected for 0 °K) which inherently provides stability due to its attractive component without requiring surface forces gives {a simple model with central forces between first neighbors together with simple three-body forces (potential depending on areas of triangles between three nearest neighbors) can reproduce the lattice constant and the three elastic moduli; here the Einstein frequency is 3.4×10^{13} sec^{-1} [K. Breuer (private communication)]}

$$\omega_E^{(M)} = (f_M/m)^{1/2} = 3.6 \times 10^{13}\ \text{sec}^{-1}\ . \qquad (10)$$

The reasonable agreement between (9) and (10) leads us to believe that despite its purely repulsive character the Born-Mayer (BM) potential together with boundary forces is an adequate description of atomic interaction in copper within a central-force model.

Corresponding to the range $r_c = 1.58D$ of the potential, the constant boundary forces due to the rest of the crystal act upon the first and second atomic layers of the surface of the crystallite. If all atoms occupy their ideal lattice sites the crystallite is in mechanical equilibrium. 3.5×10^5 cm/sec was taken as the average value of the sound velocity c in (2) [the maximum and minimum velocities in copper along low-indexed directions are 5.32×10^5 and 1.68×10^5 cm/sec, respectively (see, e.g., Ref. 8)]. Different sets of atoms were used in the investigations ranging from $3 \times 5 \times 5$ cubic cells (corresponding to 424 atoms) to $4 \times 8 \times 8$ cubic cells (1301 atoms). Results have proved to be practically insensitive to the size of the crystallite, to the elastic forces adopted, and even to drastic changes of responsive forces ($0.1 \le g \le 1$) of the surrounding medium.

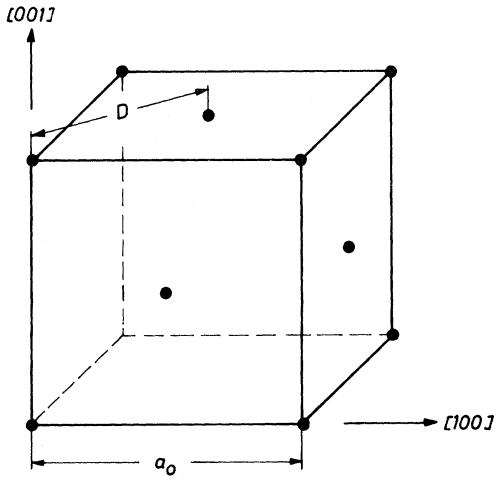

FIG. 1. Elementary cubic cell of a fcc lattice (e.g., Cu): a_0, cubic cell edge; D, nearest-neighbor distance ($= a_0/\sqrt{2}$).

III. METHOD OF COMPUTATION

Simulation of a physical event taking place in the crystallite implies solving the classical equations

of motion of all the atoms with the proper initial conditions. Rigorously speaking, the atoms should be treated as wave packets. Due to the forces exerted upon each atom by its neighbors these wave packets are believed to remain concentrated and do not spread in the course of time, as with free particles. Hence the center of the wave packet may be identified with the position of the atom. According to Ehrenfest's theorem, the center of the wave packet and also other expectation values obey classical equations. Therefore, a classical treatment of the atomic motion seems to be justified. Within a sufficiently small time interval these coupled differential equations are approximated by a corresponding set of difference equations which are solved numerically. Two standard computational methods were used alternatively: the method of the central differences and the Runge-Kutta procedure. Details are given in Ref. 6.

Tests on the accuracy of calculation were made by performing energy checks (cf. Ref. 6) after each time step. This monitors programming errors and indicates when time intervals have been chosen too large.

Two different types of computational runs have been made: "dynamical" and "static" runs. In a dynamical run one starts from mechanical equilibrium and one atom is given a certain momentum. In a static run one starts from a nonequilibrium configuration. In the latter case the potential energy is partially converted into kinetic energy. Each static run is terminated when the total kinetic energy of the crystallite falls below a certain limit, say 10^{-10} eV. This is taken as an indication of a final stable atomic-equilibrium configuration. In many cases the validity of this was checked by close inspection of the configuration of the atoms. The computer program was able to monitor atoms moving away beyond a given distance from its original site. In static runs artificial damping (aside from the action of radiation boundary forces) is used in order to hasten the attainment of mechanical equilibrium. In this artificial damping the kinetic energies of all atoms are set equal to zero when the total kinetic energy of the crystallite reaches a maximum. This process was repeated through many cycles.

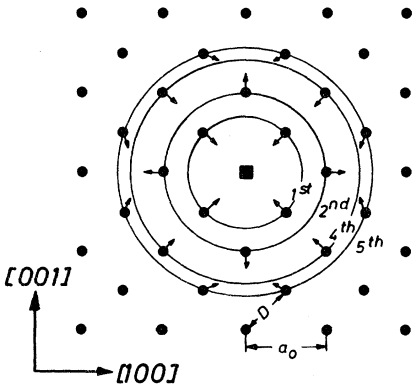

FIG. 2. Lattice relaxation around a vacancy [(010)] plane; •, ideal lattice position; →, direction of atomic displacement due to lattice relaxation; a_0, cubic cell edge; D, nearest-neighbor distance ($=a_0/\sqrt{2}$). [Circles indicate equivalent neighbors; third neighbors do not lie a (010) plane.]

TABLE I. Atomic displacements $\vec{s}$ around a lattice vacancy. (The position $\vec{r}$ of the unrelaxed atoms is given in units of $\frac{1}{2}a_0$ relative to the vacancy.)

Neighbor	r	$100(\vec{s}/\frac{1}{2}a_0)$
1st	(1, 1, 0)	(−2.54, −2.54, 0.0)
2nd	(2, 0, 0)	(+0.16, 0.0, 0.0)
3rd	(2, 1, 1)	(−0.53, −0.50, +0.70)
4th	(2, 2, 0)	(−0.9, −0.9, 0.0)
5th	(3, 1, 0)	(−0.04, −0.09, 0.0)

In all calculations a Cartesian coordinate system has been used with its axes along the principal lattice directions (parallel to the edges of the elementary cubic cell) and its origin at a corner atom of the crystallite. We have performed about one hundred runs for dynamical problems and about sixty runs for static problems.

IV. STRUCTURE OF POINT DEFECTS AND ASSOCIATED ENERGIES

A. Vacancy

Before studying dynamic events which involve point defects, it is necessary to determine the stable equilibrium configuration of these defects since all dynamic runs start from such configurations. The findings of computer calculations by other authors (cf. Ref. 5) concerning the structure and the relaxation of a vacancy have been verified: The vacancy, centered at a lattice site, has cubic symmetry. The surrounding atoms exhibit extremely small relaxations toward the vacancy. The magnitude $|\vec{s}|$ of the displacements is only $0.025D$ for nearest neighbors. Furthermore, second neighbors relax away from the vacancy, which is a well-known feature. Figure 2 shows qualitatively the structure of a vacancy in a (100) plane. Table I gives a list of relaxations up to fifth neighbors.

B. Interstitial Atom

The results of earlier calculations[5] have been confirmed also for the interstitial atom: The only stable configuration we could find is the dumbbell-

shaped split interstitial having tetragonal symmetry. Figure 3 shows qualitatively the structure of a split interstitial in a (100) plane. Table II gives a list of relaxations of the surrounding atoms.

C. Frenkel Defect

In determining the structure of a Frenkel defect (vacancy and interstitial) the following additional parameters enter: (i) the distance between dumbbell center and vacancy and (ii) the direction with respect to the dumbbell axis. Up to rather large separations between dumbbell center and vacancy all possible cases have been investigated. There is a region around each dumbbell within which a vacancy is not stable due to attractive forces between these two point defects: They recombine spontaneously and the result of such an annihilation is a perfect lattice. The region of instability comprises 74 atomic sites (see Figs. 4 and 5). This value is rather close to the result of similar calculations by Drittler *et al.*,[9] who obtained 62 unstable sites for a Morse potential as atomic interaction.

Gibson *et al.*[5] have calculated the unstable sites within a (100) plane (containing the interstitial) only. Their results agree with ours.

D. Energies Associated with Defects

The potential energies associated with the different types of defects discussed above have been calculated. These energies are taken as the differences between the potential energy of the perfect crystallite and the crystallite containing the corresponding defect in equilibrium.

We first have determined the energies associated with a vacancy or an interstitial by simply taking an atom out of the crystallite or, correspondingly, inserting an atom. Although these energies are physically not meaningful if considered independently, their sum yields the formation energy of a separated Frenkel pair. For the vacancy one atom is taken out of the perfect crystallite and moved, reversibly, infinitely far away from it. The resulting energy change is $E_V = -0.71$ eV. In order to separate the contribution of the relaxation of the lattice one proceeds in two steps. First, one atom is removed with all other atoms being fixed at their ideal sites. Then the potential energy changes by $E_V' = -0.61$ eV. [This value can also be obtained analytically by summing the energy contributions of nearest neighbors: $E_V' \approx 12V(r=D)$, where V is taken from (8). Contributions of more distant neighbors can be neglected.] If these atoms are then allowed to relax, the potential energy is lowered further by $\Delta E_V = -0.10$ eV [see Fig. 6(a)]. For the split interstitial (dumbbell) an atom far away from the crystallite is taken and, reversibly, inserted into the perfect crystallite. The resulting energy change, once the structure has been thoroughly relaxed, is $E_I = 3.50$ eV. Again, this final state can be obtained in two steps. First, all atoms eventually surrounding the dumbbell are held at their ideal lattice sites while the two dumbbell atoms are held at their final positions. (In control runs the additional atom has been inserted also at arbitrary locations. This, however, requires long calculation times because the potential energy at the beginning is extremely high.) As a result, the potential energy increases by $E_I' = 9.19$ eV. Then the lattice is allowed to relax. This relaxation is associated with a decrease of the potential energy of $\Delta E_I = -5.69$ eV [see Fig. 6(b)].

The values of E_V and E_I have been calculated for different shapes and sizes of the crystallite. They turned out to be independent of these parameters. However, E_I is slightly dependent upon alterations of the strength of the spring forces at the boundaries of the crystallite.

From these data of the separated defects (either a vacancy or an interstitial is in the crystallite,

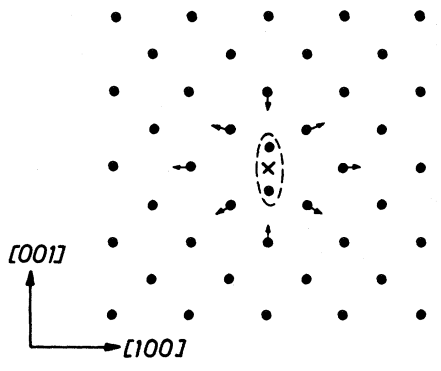

FIG. 3. Structure of split interstitial (dumbbell): •, ideal lattice position; two closed circles surrounded by dotted line, dumbbell atoms; ×, center of dumbbell; →, direction of atomic displacements due to lattice relaxation.

TABLE II. Atomic displacements $\vec{s}$ of and around a split interstitial (oriented along [001]). (The position $\vec{r}$ of the unrelaxed atoms is given in units of $\frac{1}{2}a_0$ relative to the dumbbell center.)

Atom position	$100(\vec{s}/\frac{1}{2}a_0)$
Upper dumbbell atom (see Fig. 3)	(0.0, 0.0, 60.4)
(1, 0, 1)	(+16.7, 0.0, 8.9)
(1, 1, 0)	(−4.6, −4.6, 0.0)
(2, 0, 0)	(+2.0, 0.0, 0.0)
(0, 0, 2)	(0.0, 0.0, −1.3)

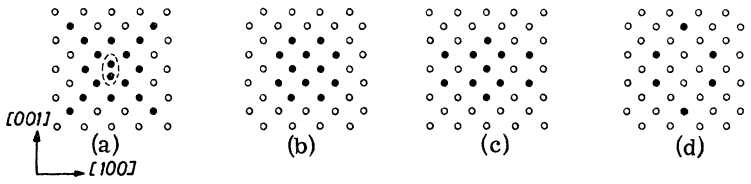

FIG. 4. Unstable lattice sites for a vacancy around an interstitial. Split interstitial is oriented along [001]. Unstable sites are indicated for each lattice plane separately: (a) (010) plane containing split interstitial; (b), (c), and (d) neighboring planes in natural order; •, unstable site; ∘, stable site.

but not both at a time), the energy of formation of an infinitely separated Frenkel pair is obtained:

$$E_{FP} = E_V + E_I = 2.79 \text{ eV} .$$

The above energy values agree well with earlier calculations.[5] Slight differences probably arise from the longer range of the interatomic potential adopted here.

We have also calculated the formation energy of a Frenkel pair for finite separation distances. For this purpose, a vacancy and an interstitial are inserted into the crystal at the same time and the energy content of the whole crystallite is computed after mechanical equilibrium has been reached. The energy difference between the perfect crystallite and the one containing a Frenkel pair, i.e., the formation energy of a Frenkel pair at a finite distance, turns out to be practically independent of this distance and also of the orientation of the dumbbell relative to the vacancy as long as the Frenkel pair is stable. This rather astounding result has to be ascribed to the strong concentration of large displacements of each point-defect structure in the immediate neighborhood of the defect center. Of course, there is an (elastic) interaction between these two point defects at any distance outside the instability volume, but this interaction energy is negligibly small compared to the energy of each point defect itself.

V. DYNAMIC BEHAVIOR OF A VACANCY

Starting from the equilibrium (cf. Sec. IV A) the vacancy can be moved by transferring kinetic energy to neighboring atoms (Fig. 7). The threshold energy for initiating a jump of the vacancy depends on the position of the knocked-on atom relative to the vacancy and on the direction of the atom's initial momentum.

The easiest way to initiate a vacancy jump is to push one of its 12 nearest neighbors directly into the vacancy (see Fig. 7, case $\alpha = 0$). The minimum energy $E(\alpha = 0)$ for this process can be roughly estimated by calculating the height of the potential barrier of the rectangular "window" which is formed by four atoms and which the knocked-on atom (starting from its initial position amidst 11 nearest neighbors) has to penetrate in order to fall eventually into the vacancy. With the potential (8) we obtain

$$E(\alpha = 0) \approx 4A e^{-D\sqrt{3}/2a} - 11A e^{-D/a}$$

$$= 1.17 \text{ eV} - 0.56 \text{ eV} = 0.6 \text{ eV} ,$$

if we use the ideal lattice positions; i.e., if we neglect lattice relaxations around the vacancy and the dynamic response of the lattice during the jump.

The computer simulation yields a value between

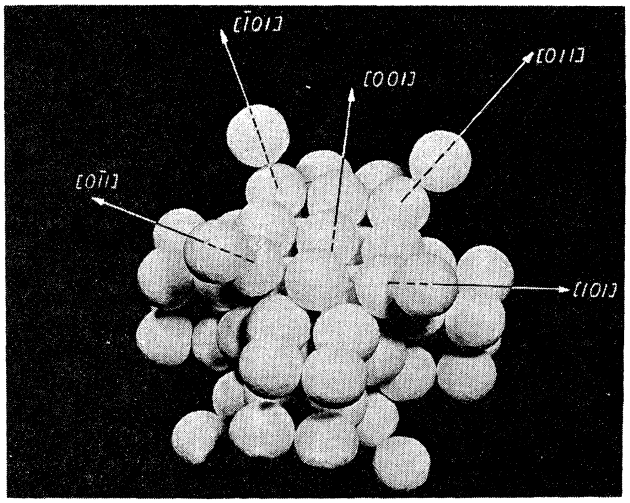

FIG. 5. Three-dimensional view of unstable lattice sites of Fig. 4. The set has fourfold symmetry about [001] direction. The {001} plane containing the center of the split interstitial is a mirror plane.

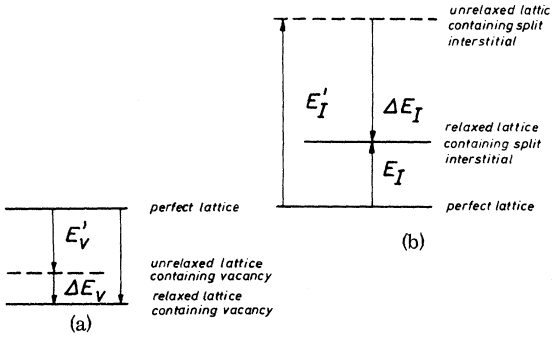

FIG. 6. Potential energies (schematic) of crystallites at different defect states: (a) case of a vacancy (one atom is taken out of the perfect crystallite and moved infinitely far away); (b) case of a split interstitial (an atom taken from infinity is inserted into the perfect crystallite).

0.55 and 0.60 eV. With increasing angle α the threshold energy increases (see Fig. 7) due to the increasing energy loss to the "window" atoms. In all cases the knocked-on atom and the vacancy interchange sites. It takes about 150 time units until the lattice essentially reaches its equilibrium again (one time unit $t_0 = 3.27 \times 10^{-15}$ sec). Second-nearest neighbors to the vacancy require such a high threshold that their contribution to inducing vacancy jumps can be neglected compared with nearest neighbors. A rough estimate analogous to the nearest-neighbor case for $\alpha = 0$ gives a threshold larger than 10 eV and one would not expect a drastic reduction of this value in the dynamic event. Computer runs have been made only up to 2.5 eV. They did not show a jump of the vacancy.

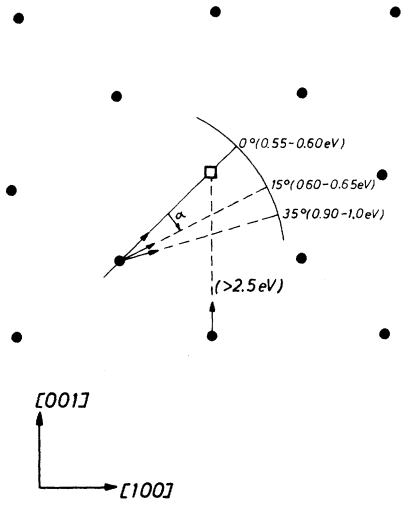

FIG. 7. Initial directions and minimum starting energies of atoms near a vacancy which lead to a vacancy jump (100 plane).

VI. DYNAMIC BEHAVIOR OF AN INTERSTITIAL ATOM

Dynamic processes of the dumbbell-shaped split interstitial start from the equilibrium configuration (cf. Sec. IV B).

In order to excite dynamic events one can transfer energy to the interstitial directly or to the neighboring atoms. In the present study we have restricted ourselves to knocking on the interstitial only. By interstitial we mean in the following either one of the two equivalent members of the dumbbell.

For *small* energy transfers only vibrations can be excited. Let us first consider the possible vibrational modes of the two dumbbell atoms. From symmetry considerations (see Table III) one finds two modes where the dumbbell center is at rest: a mode (No. 1) where the two atoms oscillate against each other parallel to the dumbbell axis (axial mode) and a mode (No. 2) where the two atoms oscillate with opposite amplitudes perpendicular to the dumbbell axis (libration mode). There are also two modes where the common mass center is vibrating: a mode (No. 3) where the mass center oscillates parallel to the dumbbell axis and a mode (No. 4) where it oscillates perpendicular to the dumbbell axis. Altogether there are six modes if degeneracy is included (see Table III). One would anticipate that the frequencies of all these modes are very high, possibly above the maximum frequency, because the force constants due to the smaller interatomic distances (as compared with the equilibrium distance in the ideal lattice) will be much higher than any in the ideal lattice. In fact, Gibson *et al.*[5] have found in their computer simulations that mode No. 1 is localized, i.e., its frequency does lie above the maximum frequency. Under the tentative assumption that the frequencies of all modes described above are localized one can approximately estimate their values: All nearest neighbors of the

TABLE III. Vibrational modes of the dumbbell. The frequencies ω_i' are values from an analytical treatment; the frequencies ω_i are computer results. (The maximum frequency is $\omega_m = 4.2 \times 10^{13}$ sec^{-1}; the time unit is $t_0 = 3.27 \times 10^{-15}$ sec.)

Mode no.	Mode	Degeneracy	ω_i' / 10^{13} sec	ω_i'/ω_m	$\frac{T}{t_0} = \frac{2\pi}{\omega_i t_0}$	ω_i/ω_m	$\frac{\lvert\omega_i - \omega_i'\rvert}{\omega_i}$
1	↕ ↕	1	5.5	1.30	33	1.37	5%
2	↔ ↔	2	3.6	0.85	37	1.25	32%
3	↕ ↕	1	1.8	0.42	≈300	≈0.15	>100%
4	↔ ↔	2	4.1	0.97	38	1.21	20%

dumbbell are considered to be fixed at their actual sites (taken from Sec. IV B) and the two dumbbell atoms vibrate within the rigid cage of these neighbors. For the potential (8) one obtains the frequencies ω_1', ω_2', ω_3', and ω_4' listed in Table III. The maximum frequency ω_m was taken approximately as the Debye frequency corresponding to a Debye temperature of 320 °K. One obtains $\omega_m = 4.2\times10^{13}\,\mathrm{sec}^{-1}$. From the ratios ω_i'/ω_m (see Table III) one can expect that the mode Nos. 1, 2, and 4 will be localized. Mode No. 3 will be not localized since ω_3' is far below ω_m.

In our computer simulation we have investigated the case of small energy transfers. Especially, we have determined the frequencies ω_1, ω_2, ω_3, and ω_4 of the above-mentioned modes, and compared them with the values from the analytical approximate treatment (see Table III). The computer values are higher than the approximate values because in the approximate treatment all neighbors are fixed, whereas in the computer simulation the neighbors vibrate in antiphase to the dumbbell atoms, thus increasing the effective force constants and, hence, the frequency (the approximate treatment can be viewed as a variational procedure taking the dumbbell displacements as variational parameter; here the variational frequencies must always be lower than the actual frequencies). Since with increasing frequency the vibrations become better localized (less participation of the environment in the vibration), also the assumption of fixed neighbors becomes better. This explains (see Table III) why with increasing frequency the discrepancy between computer values and approximate values becomes smaller.

If the interstitial starts with a momentum along the dumbbell axis ($\theta = 0°$, 180°, Fig. 8) the axial mode (No. 1) is excited. Figure 9(a) shows the variation of distance between the two dumbbell atoms vs time ($t = 0$ is the starting time). This relative motion of the dumbbell does not show any attenuation within these first 30 oscillations (of course, if pursued sufficiently long it would be attenuated in our model since our radiation forces do not become zero for $\omega > \omega_m$ as they should). The motion of the mass center is strongly attenuated [Fig. 9(b)]. Evidently, it does not show an eigenfrequency.

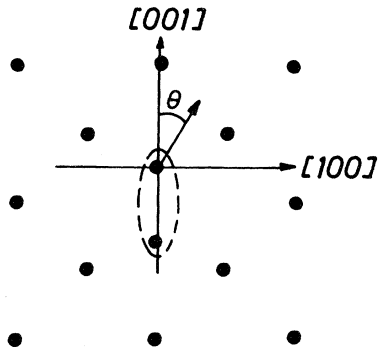

FIG. 8. Position of dumbbell at beginning of dynamic event (θ is the starting angle of the interstitial with dumbbell axis).

Figure 10 illustrates how the energy is dissipated into the vicinity of the interstitial and eventually emerges through the surface. In this case an interstitial has received 0.25 eV at the beginning. After 900 time units an energy of about 0.04 eV is still concentrated in the axial dumbbell vibration ("localized mode"), whereas about 0.08 eV are shared by all the other atoms of the crystallite. Therefore these atoms practically have come to rest. We have made many runs with initial energies ranging from 10^{-2} up to 0.35 eV without inducing jumps. These are the characteristic features which all runs have in common:

(i) About 20% of the initial energy (imparted to one dumbbell atom) is stored in the axial mode of the two dumbbell atoms. For the dumbbell with fixed environment a fraction of 50% would be transferred to the axial motion. The difference of 30% is shared by neighboring atoms participating in the localized mode. There is no attenuation to be seen within 1000 time units.

(ii) The period of the axial mode is about 33 time units (one time unit $= 3.27\times10^{-15}$ sec) and independent of energy (and amplitude). This is about 25% larger than reported in Ref. 5. The difference might be caused by a larger cutoff r_c in the present work. In order to describe this mode correctly a time step of at most two time units has to be used in integrating the equations of motion; this corresponds to at least four calculational steps per quarter cycle.

(iii) The amplitude of the axial mode goes up to 8% (maximum energy) of the equilibrium distance λ ($\lambda = 1.2a_0/2$) between the two dumbbell atoms. For such small amplitudes the dumbbell behaves as a harmonic oscillator consistent with the amplitude independence of its eigenfrequency.

(iv) The vibration of the dumbbell center is much slower than that of the localized axial mode. Its period is about 400 time units. Its amplitude mounts up to 0.3λ (for 0.35 eV) and decreases very fast due to anharmonic effects.

For starting directions off-axis ($\theta \neq 0°$, 180°, Fig. 8) we have investigated several cases in a (100) plane. The axial mode of the dumbbell is present in all cases with the same period of 33 time units as found for $\theta = 0$. In addition to the axial mode [No. 1, Table III and Fig. 9(a)] a libration mode (No. 2, Table III) is excited by the

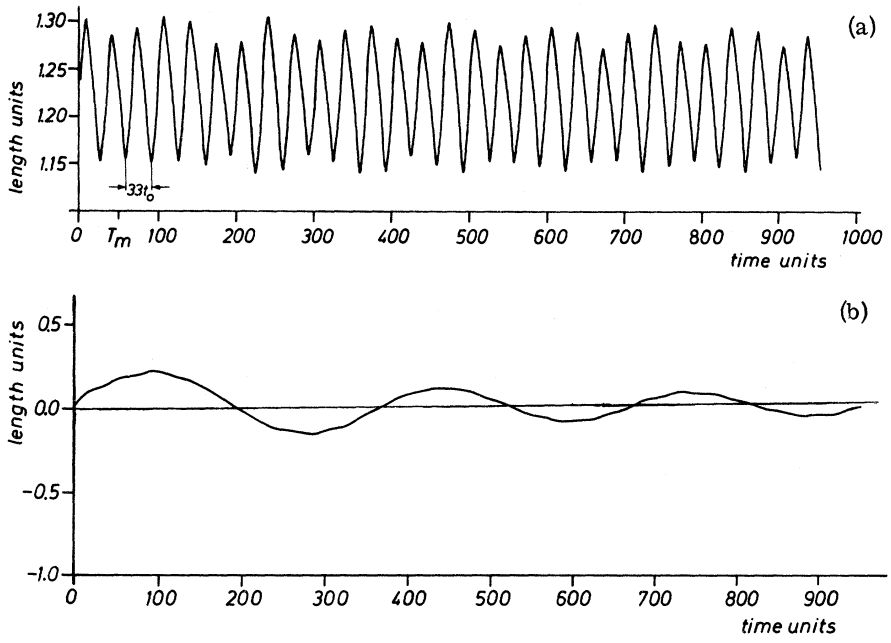

FIG. 9. Motion of dumbbell atoms (starting energy 0.25 eV): (a) relative motion; (b) motion of common mass center (time unit $t_0 = 3.27 \times 10^{-15}$ sec, $T_m = 2\pi/\omega_m = 46t_0$; length unit $l_0 = \frac{1}{2}a_0 = 1.80 \times 10^{-8}$ cm).

transversal component of the initial momentum given to the interstitial. It is superimposed upon a highly attenuated anharmonic torsional vibration of the dumbbell. Figure 11 shows typically these two angular motions. In addition to the axial component of the mass-center motion (No. 3, Table III) a perpendicular component (No. 4, Table III) is excited. In agreement with the indications from analytical calculations this normal component shows a localized mode which also comes very close to the calculated value (Table III). Again this localized mode is superimposed upon a highly attenuated low-frequency vibration. Figure 12 shows typically this mass-center motion of the dumbbell.

For *higher*-energy transfers to the interstitial not only vibrations can be excited but also a permanent rearrangement of atoms may be induced: The dumbbell structure jumps. The threshold energies for such a jump have been determined for different starting angles in a (100) plane. Figure 13 shows the threshold energies for different initial directions θ of the interstitial and also the final configurations after the jump has been completed. The time until a jump is completed is about 350 time units. Then all atoms

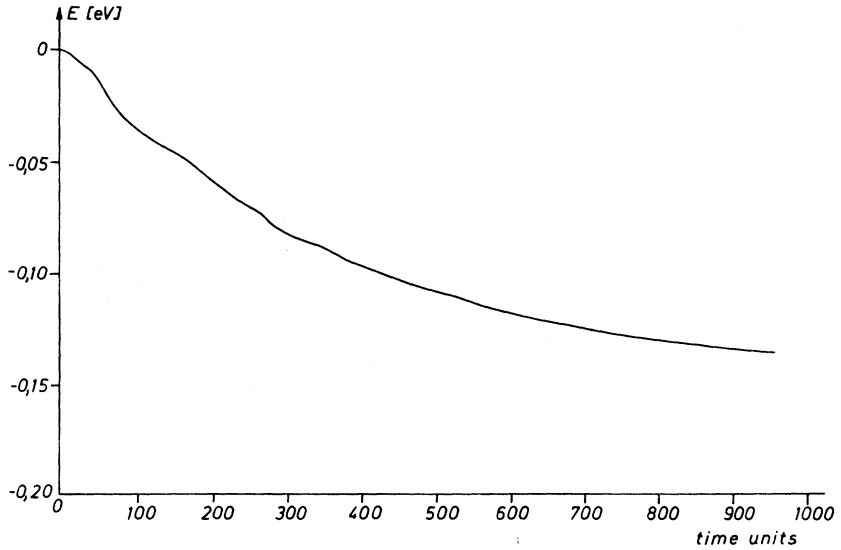

FIG. 10. Energy loss through surface of a crystallite which contains a knocked-on interstitial (starting energy 0.25 eV).

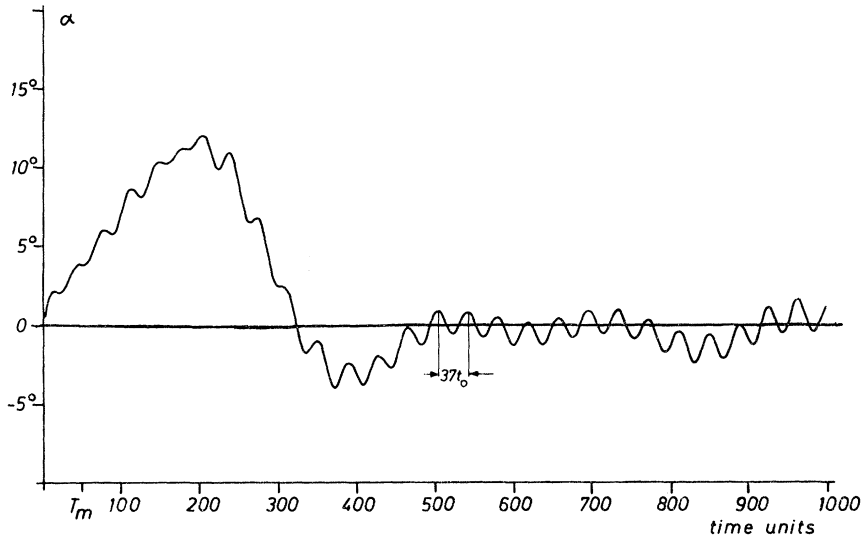

FIG. 11. Torsional vibrations of a dumbbell with starting angle $\theta = 22.5°$ and starting energy 0.25 eV. A high-frequency libration mode is superimposed upon a low-frequency anharmonic oscillation (angle α between instant dumbbell axis and initial orientation vs time).

have attained their final positions, exhibiting only vibrations about these positions. The "new" dumbbell shows the localized modes as in all cases above where the interstitial was given an energy without leading to a jump.

Among all cases under investigation there was none in which a genuine rotation of the dumbbell into another equivalent direction occurred. Every rotation (types II, III, Fig. 13) is accompanied by a translatory motion of the dumbbell. Despite the high anisotropy of the lattice the threshold energies for inducing a single step vary only by a factor of 2 between the easiest and the hardest direction. Taking a rough average value of 0.40 eV for the (100) plane and assuming it will be also representative for the unit sphere we can estimate a cross section for initiating a jump of an interstitial by energetic electrons. According to recent calculations (see Fig. 4 in Ref. 1) the cross section for an energy transfer of 0.4 eV by MeV electrons to copper atoms is about $1 \times 10^{+4}$ b, being almost independent of the incident electron energy. Since there are two equivalent atoms in a dumbbell we obtain $2 \times 10^{+4}$ b as a cross section for inducing a jump. Of course, this rough estimate provides (within this model calculation) only a lower limit because we have considered energy transfers only to the dumbbell atoms. Contributions to the cross section by knocked-on neighboring atoms might be of the same order of magnitude. It is true that more energy will be required (leading to a smaller cross section per atom) to displace the dumbbell by energy transfers to neighboring atoms but, on the other hand, there are many atoms surrounding a dumbbell.

VII. DYNAMIC BEHAVIOR OF A FRENKEL PAIR

After having investigated the dynamic behavior of a vacancy and an interstitial separately the question arises how this behavior is modified if vacancy and interstitial form a Frenkel pair.

By small energy transfers again only vibrations can be excited. As in the case of the separate dumbbell, one sees unattenuated localized modes. Even if the vacancy is very close, as in configurations which are illustrated in Figs. 14 and 15, the

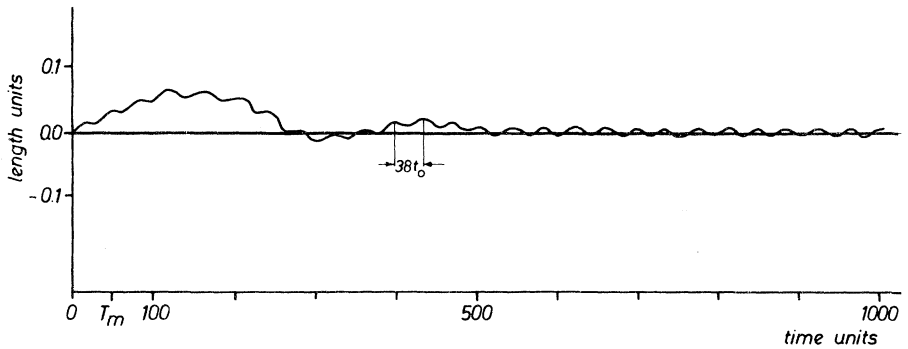

FIG. 12. Normal component of mass-center motion of dumbbell. Starting angle $\theta = 22.5°$ and starting energy = 0.25 eV (time unit $t_0 = 3.27 \times 10^{-15}$ sec, $T_m = 46\ t_0$; length unit $l_0 = \frac{1}{2}a_0 = 1.80 \times 10^{-8}$ cm).

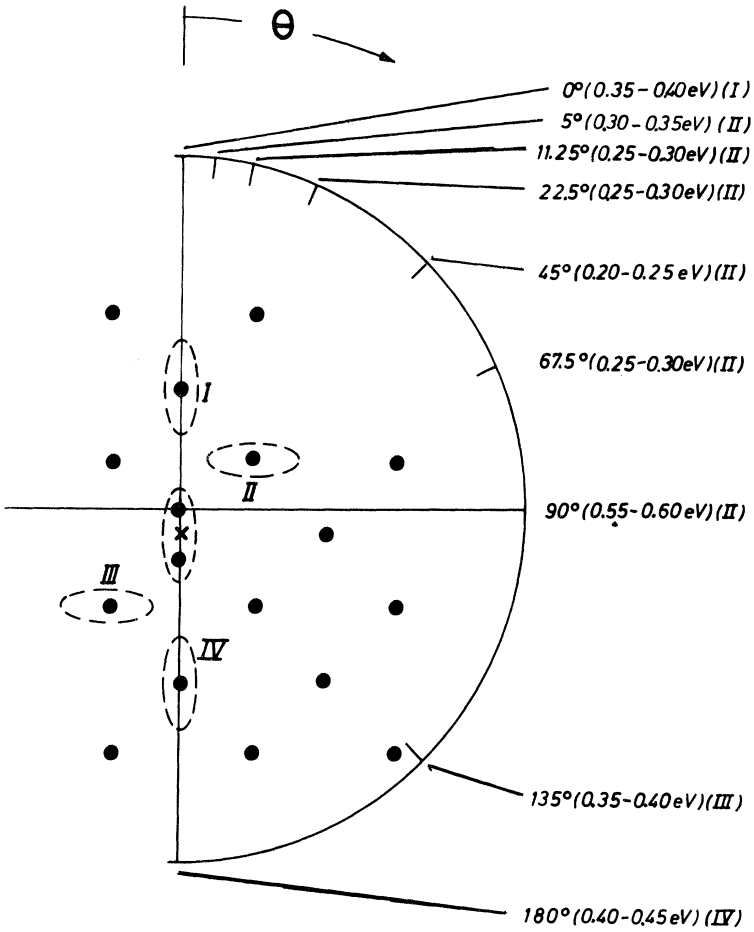

FIG. 13. One atom of the dumbbell (centered at the origin) is given a minimum energy resulting in a jump of the dumbbell configuration. This threshold energy is given for various angles θ in the (100) plane. For each value of θ, also, the final configuration (I, II, III, IV) is indicated.

dynamic behavior of the dumbbell is unaffected as long as only vibrations are excited.

At higher-energy transfers either a jump of the vacancy or the interstitial may be induced, resulting in a new configuration of the Frenkel pair, or the energy transfer leads to annihilation. Of course one has to study many initial configurations: The configuration of a Frenkel pair is characterized by the *distance* vacancy interstitial and by the *angular position* of the vacancy relative to the dumbbell axis, hence adding another multiplicity of variables to the problem. From the (static) structure of a stable Frenkel pair we have learned (see Sec. IV C) that a vacancy and an interstitial in a Frenkel pair behave as if they were separated. Thus, one would expect that the energies for a jump of either a vacancy or an interstitial would practically not be affected in any stable Frenkel-pair configuration. However, a jump is a dynamic event whose result cannot be anticipated on the grounds of static considerations. It is not even possible to predict whether the threshold for an interstitial jump with a vacancy present is smaller or larger than without a vacancy. In fact, this depends on the particular Frenkel-pair configuration. Figures 14 and 15 illustrate two specific examples. One of these (see Fig. 14) is a configuration where the threshold for a dumbbell jump in the axial direction towards a vacancy amounts to 0.75 eV. Without vacancy a jump requires only 0.4 eV. Thus, due to the presence of a vacancy the threshold energy *increases* by a factor of 2. In the second example (Fig. 15) the vacancy is a little off the dumbbell axis. The threshold for a dumbbell jump in this case is 0.08 eV with a vacancy present, and about 0.35 eV without vacancy; i.e., the presence of a vacancy *lowers* the energy threshold by a factor of 4. In both examples the dumbbell jump results in the annihilation of the Frenkel pair. It might well be that jumps which do not lead to annihilation require a minimum energy which is independent of the presence of a vacancy. The annihilation of a Frenkel pair is a rather dramatic event: The relatively small threshold energy (of about 0.1 eV) triggers the release of a large fraction (> 1 eV) of the large potential energy stored mainly in the dumbbell. Figure 16 shows the sudden in-

crease of kinetic energy in the crystallite when the dumbbell starts to decay into the vacancy.

A further and more systematic investigation of vacancy jumps and interstitial jumps within a Frenkel pair is continuing.

Recently Drittler *et al.*[9] have in a similar study investigated threshold energies of Frenkel-pair annihilation induced by low-energy transfers using a Morse potential and a smaller crystallite. At the present state our results cannot be compared with theirs since they have investigated different Frenkel-pair configurations. However, they have found also energy thresholds of about 0.1 eV for annihilation.

VIII. DISCUSSION AND COMMENTS

The results presented in this paper have to be scrutinized from two points of view: a numerical one and a physical one.

The numerical calculations have been performed with high precision. Truncation errors are negligible. A large number of checks such as analytical control calculations, energy conservation, and variation of time steps in the integration processes rule out serious numerical errors. A principal error might arise from using a discontinuous force function dV/dr [cf. Eq. (6)] in integration schemes, such as Runge-Kutta, which actually require continuous functions even up to higher derivatives. We are rather confident, also, that such an error is negligible, since the step height of dV/dr is very small. In addition, the checks mentioned above should have indicated such an error.

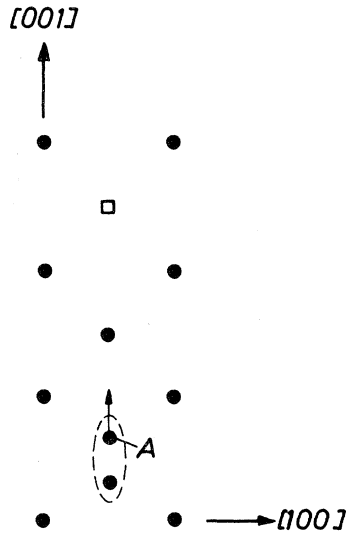

FIG. 14. Frenkel-pair configuration (schematic) in a (100) plane, where dumbbell atom A starts toward the vacancy (see text).

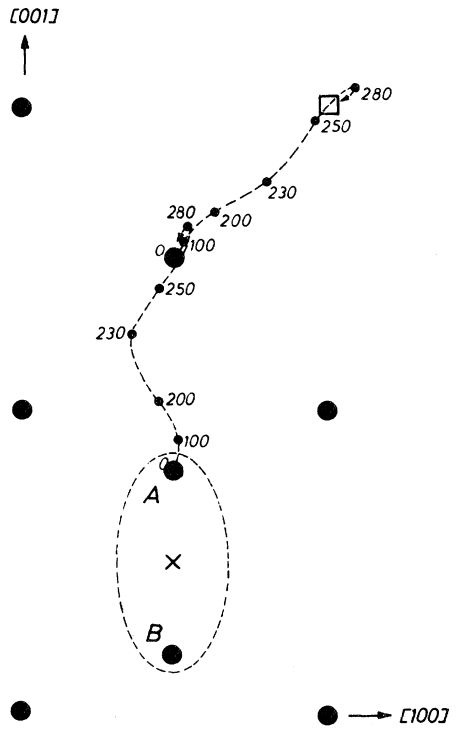

FIG. 15. Trajectories of atoms involved in annihilation of a Frenkel pair. [Dumbbell atom A starts with 0.10 eV under 11.25° off-axis at $t=0$. The numbers along the trajectories indicate the time (in time units) for different positions. Dumbbell atom B eventually takes the position (×) of the initial dumbbell center.]

The main critique of this, as with any computer simulation of dynamic events in a crystal lattice, will focus on the physical model. First we have approximated the response of the infinite rest crystal by boundary forces at the crystallite. These boundary forces have been varied within a wide range. All results are practically not influenced by the choice of the force constants, as long as the size of the crystallite is sufficiently large. (The force constant of the radiation forces affects only the rate of energy loss, i.e., the time until the kinetic energy of the crystallite has dropped to essentially zero.) Indeed, we encountered some cases in which the crystallite was too small and its size had to be increased. As an example, the energy threshold for a dumbbell jump in axial direction in a crystallite containing $3\times3\times8$ cubic cells turns out to lie between 0.45 and 0.50 eV, whereas with $5\times5\times7$ and more cubic cells this value approaches 0.35–0.40 eV. Fortunately, due to the small energies used in subthreshold collisions, rather small atomic sets are sufficient. In addition, jumps take place within times smaller than those required for a back reaction of the boundary if the defect is sufficiently far away. All

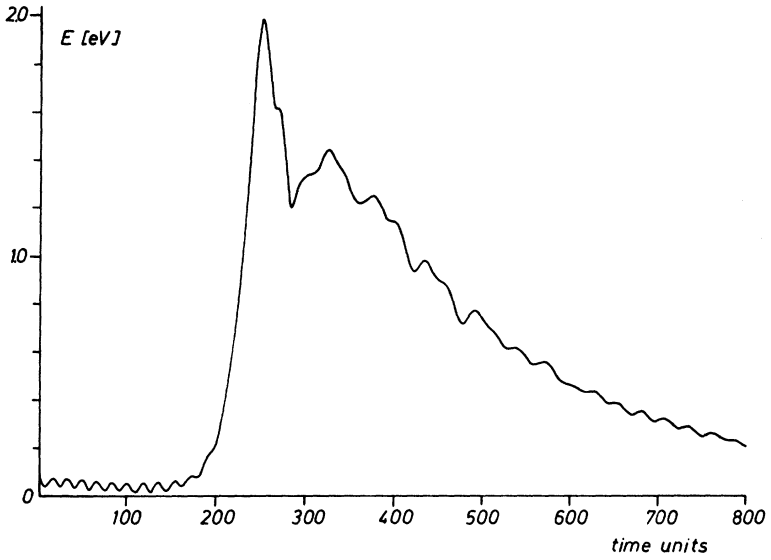

FIG. 16. Kinetic energy of crystallite containing a Frenkel pair before and after annihilation ($t \approx 170 t_0$: onset of decay of dumbbell; run as in Fig. 15).

results given in this paper stem from runs on sufficiently large crystallites.

Next, no thermal vibration of the lattice atoms has been included. This is probably a rather severe restriction in all static runs, e.g., for determining the instability volume of a Frenkel pair. But also with dynamic events the absence of thermal vibration may influence the results: It is true that dynamic events are accompanied by a strong lattice agitation simulating in some sense thermal vibration. However, this agitation is fading away much too quickly to provide a substitute for the many vibrational modes which are present in a real crystal within a time span corresponding to the duration of a dynamic event. At the present state no general predictions can be made as to how the inclusion of thermal vibration will change the results given here. It is one of the objectives of our future work to investigate the influence of thermal vibrations with the ultimate goal of simulating temperature-dependent recovery of close Frenkel pairs.

Presumably, the most serious reservation against the model concerns the atomic interaction. We have adopted the same two-body central repulsion between atoms together with a constant surface force as did Gibson *et al.*[5] A recalculation of many of their results provided us with many thorough checks on our new computer program, which will be used for more and similar studies in the future. In principle, a two-body force is a rather poor description of atomic interaction in a metal for small kinetic energies (as in our runs here). Even at higher energies the picture of two-body forces does not become better if an event has to be followed until its end, because all eventual processes are determined by small energies. For instance, in producing a stable Frenkel pair the interstitial has to reach a final position outside the instability region. Whether or not a final position is stable will be determined in the low-energy part of the history where the tail of the interatomic forces and the cohesive forces are important. Thus even threshold energies as high as 25 eV for damage production depend on forces which possibly are not of a two-body type.

Nevertheless, there seems to be hope that an effective two-body force is a rather good description of atomic interaction in the particular case of copper (and in similar metals) where ionic cores are large. This was pointed out by DeWette *et al.*,[7] who successfully employed a Morse potential in lattice-dynamical calculations for a perfect copper crystal. This opinion is supported by our findings that the local response as checked by calculating the Einstein frequency for a Born-Mayer potential has the right order of magnitude. It might be that in a copper crystal containing point defects, where smaller interatomic distances occur (e.g., as in an interstitial structure), a two-body force is an even better description of the atomic interaction than in a perfect crystal. We plan to extend the present investigation by involving such a potential which in addition to the merits just mentioned makes the lattice inherently stable, i.e., without applying constant surface forces for reasons of stability. There is some indication that our calculations, if repeated with a suitable Morse potential, will have about the same results as with a Born-Mayer potential together with constant surface forces, because recent investigations[9] with a Morse potential yielded about the same number of unstable Frenkel-pair configurations as in our calculations (cf. Sec. IV C) and, furthermore,

also the displacements of nearest neighbors of a split interstitial are comparable.[10] We have made some preliminary runs with a Morse potential: The structure of interstitial and vacancy are practically the same as in this paper and the axial mode turns out to have a slightly higher frequency than with the Born-Mayer potential.

Recently, several authors[11-13] have investigated the influence of specific properties of various adjusted (two-body) interatomic potentials upon point-defect calculations. Unfortunately, their very detailed studies did not include the sensitivity of these calculations to the rather restrictive boundary conditions: In one case[12] the computational cell of atoms was imbedded in an *isotropic* elastic continuum and in the other case[11] the movable atoms of a crystallite were surrounded by a mantle of immovable atoms. Thus, at the present state of the art there is really no interatomic potential which has a preference for physical reasons. Unfortunately, there are no experimental data available to be compared directly with any of the atomistic data calculated in this paper. There is some hope for determining the structure of single point defects by diffuse x-ray scattering. It would be equally challenging to measure the frequency of localized modes.

ACKNOWLEDGMENTS

We gratefully acknowledge stimulating discussions with K. Breuer, K. Dettmann, K. Drittler, G. Leibfried, M. T. Robinson, H. Wollenberger; and especially W. Schilling, who initiated this investigation. We are indebted to G. Leibfried also for a very careful reading of the manuscript.

---

[1]F. Dworschak, C. Lehmann, H. Schuster, H. Wollenberger, and J. Wurm, in Proceedings of the International Conference on Solid-State Physics Research with Accelerators, Brookhaven National Laboratory, BNL Report No. 50083-C52, 1967, p. 327 (unpublished).

[2]G. Duesing, W. Sassin, W. Schilling, and H. Hemmerich, Crystal Lattice Defects 1, 55 (1969).

[3]H. Wollenberger, in *Vacancies and Interstitials in Metals*, edited by A. Seeger *et al.* (North-Holland, Amsterdam, 1970), p. 215.

[4]G. Duesing, H. Hemmerich, W. Sassin, and W. Schilling, Crystal Lattice Defects 1, 135 (1970).

[5]J. B. Gibson, A. N. Goland, M. Milgram, and G. H. Vineyard, Phys. Rev. 120, 1229 (1960). For references pertaining to similar studies see J. R. Beeler, in *Physics of Many-Particle Systems*, edited by E. Meeron (Gordon and Breach, New York, 1966), p. 1.

[6]A. Scholz, Kernforschungsanlage Jülich, Report No. Jül-635-MA, 1970 (unpublished).

[7]F. W. DeWette, R. M. J. Cotterill, and M. Doyama, Phys. Letters 23, 309 (1966).

[8]E. Eisenriegler, Crystal Lattice Defects 2, 181 (1971).

[9]K. Drittler, H. J. Lahann, and H. Wollenberger, Radiation Effects 2, 51 (1969).

[10]K. Drittler (private communication).

[11]A. DePino, Jr., D. G. Doran, and J. R. Beeler, Jr., Radiation Effects 3, 23 (1970).

[12]R. A. Johnson, Radiation Effects 2, 1 (1969).

[13]E. Ehrhart, Kernforschungsanlage Jülich, Report No. Jül-810-FF, 1971 (unpublished).

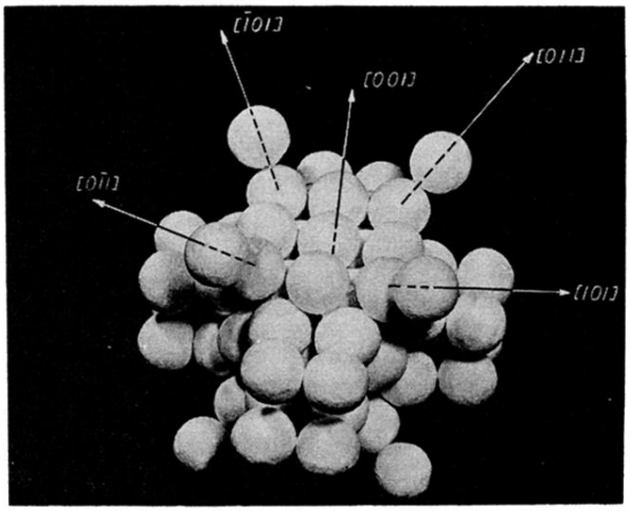

FIG. 5. Three-dimensional view of unstable lattice sites of Fig. 4. The set has fourfold symmetry about [001] direction. The {001} plane containing the center of the split interstitial is a mirror plane.